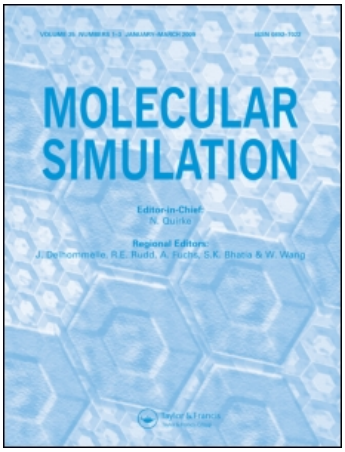

Molecular Simulation
Publication details, including instructions for authors and subscription information:
http://www.informaworld.com/smpp/title~content=t713644482

Hydrogen dissociations on small nickel clusters

B. Liu[a]; M. T. Lusk[b]; J. F. Ely[a]
[a] Chemical Engineering Department, Colorado School of Mines, Golden, CO, USA [b] Physics Department, Colorado School of Mines, Golden, CO, USA

To cite this Article Liu, B. , Lusk, M. T. and Ely, J. F.(2009) 'Hydrogen dissociations on small nickel clusters', Molecular Simulation, 35: 10, 928 — 935
To link to this Article: DOI: 10.1080/08927020902912279
URL: http://dx.doi.org/10.1080/08927020902912279

Molecular Simulation
Vol. 35, Nos. 10–11, September 2009, 928–935

Taylor & Francis
Taylor & Francis Group

Hydrogen dissociations on small nickel clusters

B. Liu[a]*, M.T. Lusk[b] and J.F. Ely[a]

[a]*Chemical Engineering Department, Colorado School of Mines, Golden, CO 80401-1887, USA;* [b]*Physics Department, Colorado School of Mines, Golden, CO 80401-1887, USA*

(*Received 15 December 2008; final version received 17 March 2009*)

The relation between geometry and nickel reactivity was explored using density functional theory. The reactivity was gauged by hydrogen and methane dissociations on atomic nickel and the tetrahedral clusters where binding energies and dissociation barriers were calculated. The results were then compared to Ni_{13} icosahedral clusters and (1 1 1) crystal surfaces.

Keywords: density functional theory; catalysis; hydrogen dissociation; nickel cluster; dissociation barrier

1. Introduction

Catalysis is undoubtedly one of the most exciting and intensively studied areas in chemical engineering. Aside from the intrinsic chemical properties possessed by catalytic materials, size and geometry can also influence the reactivity of a material. It is known that an extremely finely dispersed system does not just increase the reaction specific surface areas, but can also alter the behaviour of chemically inert materials. For example, gold nano-particles supported on TiO_2 are highly active catalysts for the oxidation of CO [1]. Also gold reactivity appears to peak at nano-particle diameter of 3 nm, another indication of a critical size effect.

Other examples include the work done by Tian et al. [2] and Narayanan et al. [3] on platinum nano-particles that demonstrated improved reactivity on certain systems. A high percentage of sites on cluster edges and at corners is believed to be responsible for the enhanced reactivity. This was shown by Narayanan's experiments, where the catalytic activities of nano-particles with tetrahedral, cubic and spherical shapes vary significantly and reaction rates increased exponentially with the number of edges and corners.

This paper presents work conducted to understand how hydrogen and methane behave in the presence of nano-scale nickel systems where nickel is in its atomic form as well as the tetrahedron formed by four nickel atoms. The purpose is to use density functional theory (DFT) electronic structure calculations to investigate the effect of cluster surface geometry on the decomposition of both hydrogen and methane. Another goal is to establish a link of hydrocarbon dissociation reactivity for these small nickel systems with respect to bigger ones, such as Ni_{13} icosahedral cluster and Ni(1 1 1) crystalline surfaces [4].

2. Methods

DMol^3 [5,6] was used to perform all the electronic structure calculations where the GGA-PW91 functional [7,8] was used to account for electron exchange and correlation energies. All calculations were spin-unrestricted to capture the magnetic properties of nickel [9]. The double numerical plus polarisation basis [5] was applied to H, C and Ni where a polarisation d-function is used on all non-hydrogen atoms and a polarisation p-function added to all hydrogen atoms. For Ni, this basis set is coupled with A norm conserving, semi-core pseudopotential [10], which can accurately describe the relativistic effects. This setup was validated against other methods using large basis sets and equivalent effective core potentials. Although all these DFT methods also indicated a tendency to overestimate the ionisation energy, consistency among the DFT calculations was achieved.

The convergence criteria for the energy, maximum force and maximum displacement tolerances were set at 2.0×10^{-5} Hartree (Ha), 4.0×10^{-3} Ha/Å and 5.0×10^{-3} Å, respectively, for all molecules and clusters. Convergence was declared for SCF iterations when at least two of the above tolerances were satisfied. No symmetry was imposed on clusters. To help convergence, spin density mixing and a thermal smearing value of 5.0×10^3 Ha were used. Although values were slightly different depending on the specific case under investigation, differences resulting from the various charge and spin mixing values used were negligible. Direct inversion of iterative subspace (DIIS) is used for all calculations set at the default value. Details on DIIS can found in reference [11]. The orbital cut-off quality was set to be fine (4.5 Å) and the multipolar expansion was set to the default value (octupole).

*Corresponding author. Email: biliu@mines.edu

ISSN 0892-7022 print/ISSN 1029-0435 online

DOI: 10.1080/08927020902912279
http://www.informaworld.com

During a transition state (TS) search, the complete linear and quadratic synchronous transit method (LST/QST) search protocol was used. The convergence tolerance was set to be medium and a root mean square convergence of 0.01 Ha/Å was used. A default maximum QST step of five was adopted and for TS optimisation, a maximum step size of 0.3 Å (default) was used.

3. Results and discussion

3.1 H—H, C—H bond breaking by atomic nickel

The investigation starts with Ni hydride molecules (both NiH and NiH_2) which are somewhat deceiving when dealing with their electronic structures and geometries. DMol[3] calculations of NiH lead to the conclusion that the stable molecule is in the doublet state (one Ni s electron bonds with H leaving one unpaired electron). The orbital occupied by this unpaired electron is identified to be playing a non-bonding role. Other theoretical studies [12,13] have found that the NiH ground state involves the triplet $3d^9 4s$ state of nickel. The partial density of states (PDOS) of s and d orbitals of the nickel and hydrogen atom plotted in Figure 1 show the electronic states before and after bonding with a hydrogen atom. The bonding between the Ni s orbital with hydrogen atom can be clearly seen. Figure 1 also semi-quantifies the interactions between nickel d-z^2 orbital with hydrogen, which has not been discussed in previous studies. In particular, the d orbital appears to be a little more dispersed (broader energy span) after Ni—H bonding. The Ni—H bond lengths in NiH hydride calculated with different DFT functionals are

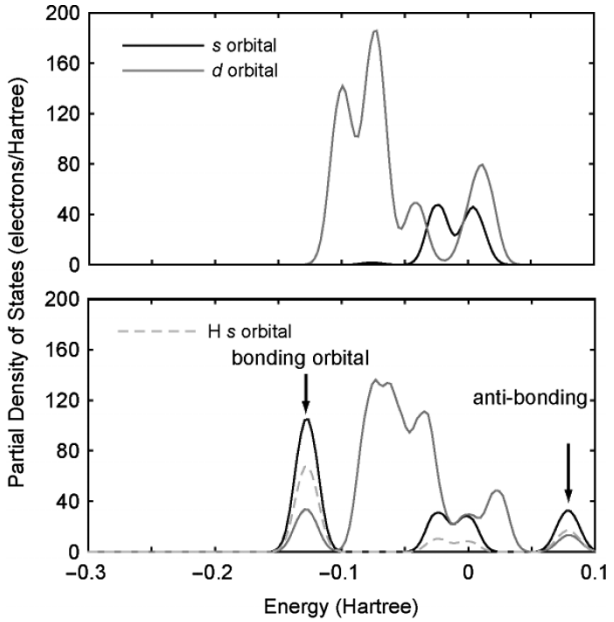

Figure 1. PDOS of nickel's s and d bands before (a) and after (b) the bonding with H.

Table 1. Ni—H bond lengths calculated from different functionals.

Functionals	Bond lengths (Å)
LDA PWC	1.43
GGA PBE	1.45
GGA PW91	1.45
B3LYP[b]	1.51
B97-1[b]	1.52
Experiment	1.48–1.64[a]

[a] See reference [26]. [b] Calculations were performed using Jaguar [14].

tabulated in Table 1. The GGA-PW91 performance is comparable to GGA-PBE, and GGA methods seem to perform slightly better than LDA-based functionals even though they all fell short of the experimental values, as hybrid functionals are not available in DMol[3]. The calculations were conducted under Jaguar [14]. Hybrid functionals, such as B3LYP and B97-1, were used. It turned out that these functionals are a little superior by giving a Ni—H bond length agreeing better with the experimental measurement.

When a second H atom approaches NiH to form HNiH, there is a general agreement that the molecule's ground electronic state is consistent with the $3d^8 4s^2$ configuration for nickel [12,13]. Earlier results of Guse et al. [12] point out that the ground state HNiH is a triplet state and has a linear geometry. Blomberg and Siegbahn [13,15] later discovered another state with a bent geometry and a $3d^9 4s$ configuration for nickel. The H—Ni—H angle is predicted to be approximately 50°. Even so, Blomberg, Siegbahn and subsequent studies [13,15–17] show that the global ground state for HNiH molecule is still the linear triplet state with an energy that is 30 kcal/mol lower than the bent singlet state [13,15]. This claim is strongly questioned by a matrix infrared study which provided evidence that the singlet state can be experimentally observed [18], and the H—Ni—H angle should be about 90° in accordance with d orbital orientation. Calculations performed by Barron et al. [19] using density functional theory confirmed the experimental observation and indicated that linear state was mistakenly identified as NiH_2's ground state because Hartree–Fock methods were used which neglect electron correlation. By including electron correlation, Barysz

Table 2. Geometries of NiH_2 molecules.

	Functionals	R_{Ni-H} (Å)	H—Ni—H (°)
Singlet	GGA-PW91	1.44	90.1
	B3LYP	1.42	87.6
	B97-1	1.42	89.6
Triplet	GGA-PW91	1.55	180.0
	B3LYP	1.57	180.0
	B97-1	1.58	180.0

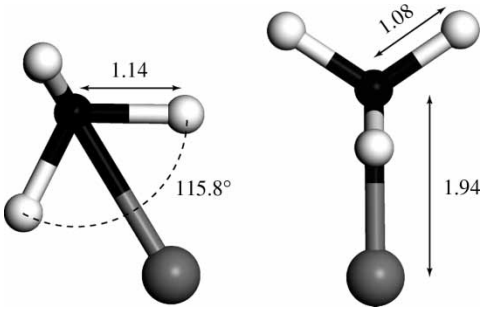

Figure 2. Geometry of CH_4 binding to a single nickel atom.

and Papadopolous [20] reached the same conclusion as Barron did.

In our study, instead of bringing a H atom to NiH, we let the nickel atom approach an intact hydrogen molecule to generate NiH_2. Calculations were performed at several distances (5.5, 2.3, 2.2 and 2.1 Å). There is a small reaction barrier of ~3 kcal/mol along the path and we found that a three-membered ring of H and Ni atoms is formed at any distance shorter than 2.1 Å. The heat of this reaction is −26 kcal/mol. Eigenvalues obtained for NiH_2 consistently show that it is a closed-shell molecule (singlet). The linear NiH_2 molecule, on the other hand, is triplet and is 8 kcal/mol higher in energy than the bent structure. Geometries for bent and linear structures are listed in Table 2, respectively. Again we compared the DMol[3] results with that from calculations hybrid functionals, the optimised molecular geometries show better agreement.

The bonds between Ni and H in nickel hydride are covalent in nature in that they take the form of sp hybridisations. Remarks have been made about the bonding between Ni and H [12] which was one of the motivations behind this study. Bond [21] pointed out that chemisorption on surfaces arise from adsorbates being covalently bonded to the surface local sites. The function of a nickel d orbital during chemisorption is intriguing. Figure 1 indicates that d electrons do participate in the bonding at some level. Dowden [22] mentioned in that during surface adsorptions, the role of d electrons is usually to induce a *chemisorption precursor state* which helps lower the activation barrier. In the case of nickel hydride, the H—H bond (0.74 Å) is stretched (to 2.03 Å) and weakened. Even though hydrogen atoms still bind to each other, the distortion of the H—H bond in the mere presence of nickel atoms makes the energy barrier for breaking two hydrogen atoms very small. More discussion on d electrons will be presented in following sections.

Bringing a nickel atom to methane does not change the structure of methane molecule appreciably shown in Figure 2. Instead, methane is molecularly bonded to the nickel atom. Unlike the directionless character of hydrogen s orbitals, sp^3 hybridisation allows methane to bond only along certain directions. We found that by bringing a Ni atom into CH_4, two C—H bonds in the molecule stretched from 1.10 to 1.14 Å, while the other two C—H bonds contracted to 1.08 Å. The Ni—C bond length is 1.94 Å.

Analogous to nickel hydrides, H—Ni—CH_3 also possesses two configurations, i.e. linear (triplet) and bent (singlet). Table 3 lists the geometries of these two molecules as well as their atomic charges. The linear geometry is approximately 10 kcal/mol higher in energy than the bent geometry. In this work, H—Ni—C_2H_5, H—Ni—C_3H_7 and H_3C—Ni—CH_3 have also been studied and bent geometries with singlet states are found to be universal in this type of system as summarised in Table 3 as well.

The C—H bond breaking and Ni—C, Ni—H bond formation between a nickel atom and methane do not occur spontaneously, hence, it is appropriate to consider that nickel has to be inserted between a C—H atom pair in order to break it. To test this, the LST–QST technique was applied to find the activation barrier. The geometry in Figure 2 was chosen as the reactant state, whereas the bent H—Ni—CH_3 was chosen as the product state.

Table 3. Geometries and Mulliken populations (for methane) for Ni hydrocarbon complex molecules.

	R_{Ni-H} (Å)	R_{Ni-C} (Å)	H—Ni—C (°)	q_{Ni}	q_C
H—Ni—CH_3 PW91	1.414	1.824	95.8	0.251	−0.077
B3LYP	1.424	1.845	96.4	0.114	−0.495
B97-1	1.430	1.850	95.4	0.147	0.547
H—Ni—CH_3 PW91	1.529	1.946	180.0	−0.499	0.335
B3LYP	1.562	1.972	179.4	0.373	−0.604
B97-1	1.572	1.968	179.3	0.391	−0.658
H—Ni—C_2H_5	1.417	1.828	99.5	–	–
H—Ni—C_3H_7	1.417	1.828	98.8	–	–
H—Ni—C_4H_9	1.415	1.832	96.8	–	–
H_3C—Ni—CH_3	–	1.824	107.2	–	–
H_3C—Ni—C_2H_5	–	1.840	104.6	–	–
H_5C_2—Ni—C_2H_5	–	1.842	105.1	–	–

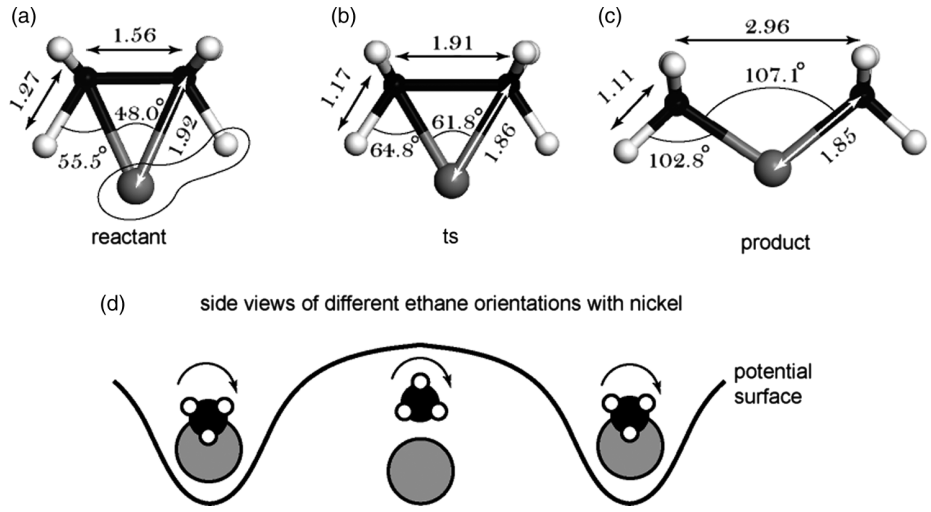

Figure 3. The reactant (a), product (c) and transition states (b) of nickel insertion into C—C bond of ethane and the interactions of ethane with nickel at different orientations (d).

The insertion is exothermic by 10 kcal/mol and the barrier to this nickel insertion is 1.36 kcal/mol. The negative imaginary frequency associated with TS is $-702\,\mathrm{cm}^{-1}$. At the TS, the C—H is further stretched to 1.38 Å, while the Ni—C distance becomes 1.86 Å.

Blomberg et al. [23] investigated the insertion of a nickel atom into a C—H bond of methane using the Hartree–Fock method and found the barrier to be 54.1 kcal/mol. Both reactions were also found to be quite endothermic, 20.7 kcal/mol. Calculations performed using density functional theory by Burghgraef et al. [24] led to results that are much closer to this study. The barrier and reaction energy were found to be 9.70 and −8.13 kcal/mol. However, the difference in Burghgraef's work is that the nickel atom was inserted in the direction of the C_{3v} symmetry axis, while in our work the nickel moves on the D_{2h} symmetry plane where we started with a more reasonable initial insertion state.

The insertion of nickel into C—C bond was studied using an ethane molecule (C_2H_6). The insertion barrier is

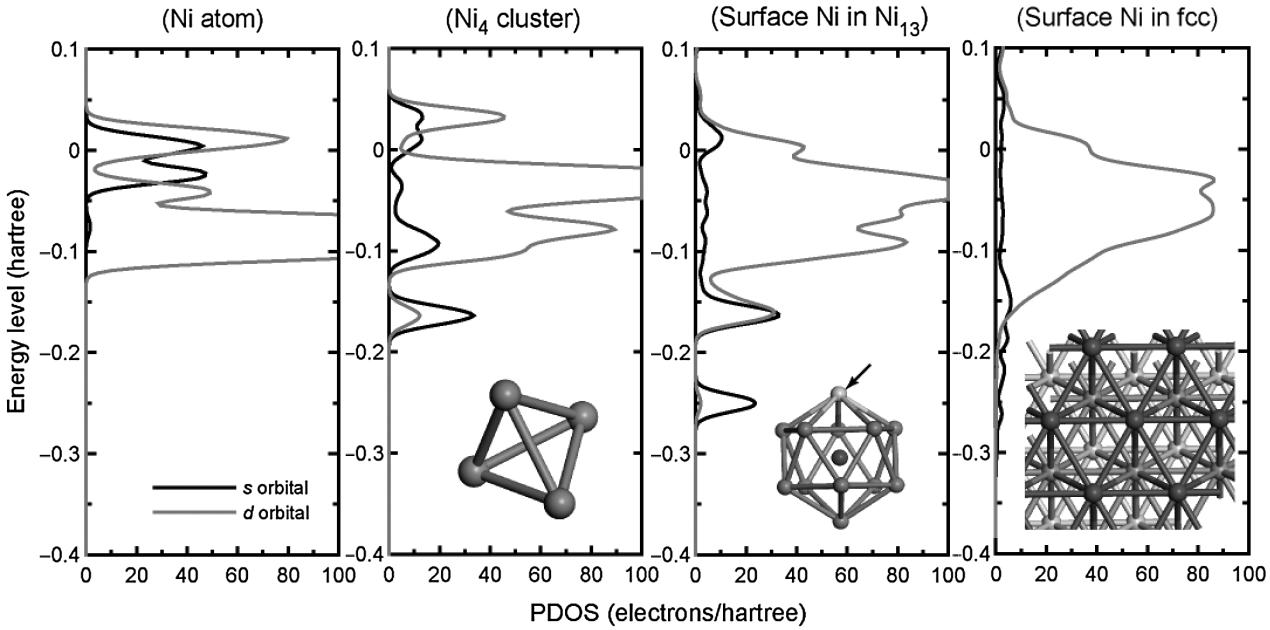

Figure 4. Partial density of states for isolated nickel, nickel in Ni_4 tetrahedral cluster, Ni_{13} icosahedral cluster and atom on Ni(1 1 1) surface, respectively.

Table 4. Binding energies of H and CH_3 on Ni_4 clusters, in kcal/mol.

Adsorption site	H	CH_3
t_1	67	62
b_2	70	56
c_3	62[a]	36[a]

[a] Binding at c_3 sites for both H and CH_3 are not stable and tend to transform to adsorptions at b_2 sites, therefore values shown here can only be considered metastable.

5.6 kcal/mol and the insertion energy is -29.6 kcal/mol. The imaginary frequency is $-976\,cm^{-1}$. When choosing the reactant state, it was found that there is one configuration that allows the binding between ethane and nickel illustrated in Figure 3(a) where H—C—Ni—C—H forms a zigzag geometry. It is believed that the interactions between H and nickel (indicated with circles in Figure 3(a)) play a significant role in stabilising the entire structure.

3.2 Hydrogen and methane dissociation on Ni_4 tetrahedral clusters

The Ni_4 tetrahedral cluster which is the most stable configuration for a four-atom system was studied next. The tetrahedron is also the first cluster that can be built in three-dimension and a basic building block of larger clusters, where the four atoms occupy the vertex (t_1 site) forming six edges (b_2 site) and four triangular facets (c_3 site). The average Ni—Ni bond length (distortion due to Jahn–Teller effects [25]) is 2.3 Å, the angle formed by two cluster facets is 70.5° and the angle between one facet and an edge is 54.8°. Geometry-wise, the icosahedral Ni_{13} is *flatter*, as

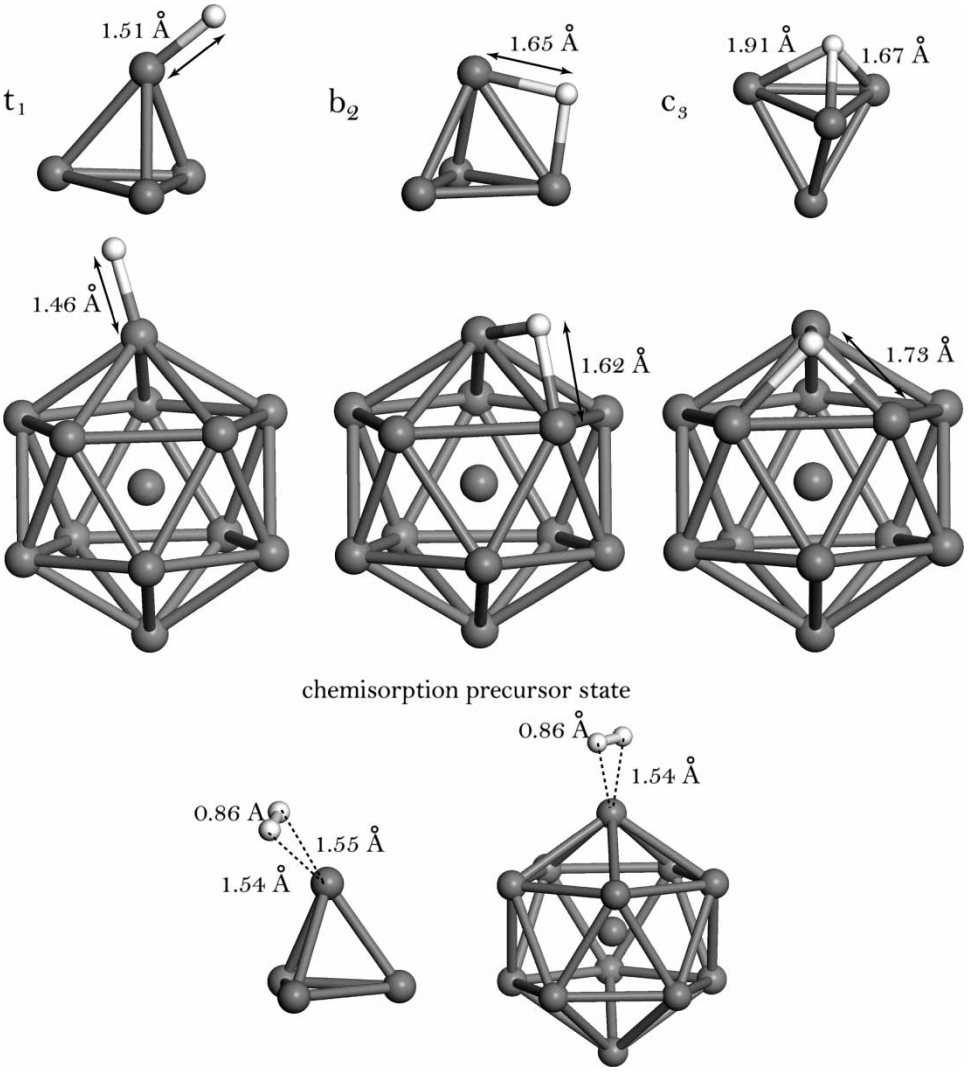

Figure 5. The adsorption of H on the t_1, b_2 and c_3 site of Ni_4 and the icosahedral Ni_{13} cluster. The chemisorption state of H_2 on these two clusters are also shown.

its corresponding angles are 138° and 110°, respectively, and the surface Ni—Ni bond length is 2.34 Å.

The PDOS of an atom in Ni_4 cluster was calculated to show the evolution of electronic structures as the system size and geometry change. An examination of this Ni_4 cluster shows that there are four singly occupied orbitals for Ni_4 clusters, three of them are responsible for the anti-bonding and one (occupying the HOMO) is non-bonding. For better comparison, the PDOS of atomic nickel, Ni_{13} icosahedral and Ni(1 1 1) surface are also included in Figure 4, which illustrates the evolution of s and d orbitals as nickel's coordination number increases. For isolated atomic nickel, the 4s and 3d orbitals show sharp and distinct peaks confined in 0 to −0.1 Ha energy span. The s orbital shifts down to −0.1 to −0.2 Ha for Ni_4 cluster, and −0.3 to −0.4 Ha for Ni_{13} cluster. Meanwhile, both s and d orbitals become more and more dispersed by populating over much broader energy spans, a characteristic of metal in crystals form.

The energetics of hydrogen and methyl adsorptions on Ni_4 were studied by placing H and CH_3 at t_1, b_2 and c_3 site of Ni_4 cluster, respectively, and the binding energies are listed in Table 4. Figures 5 and 6 illustrate the optimised binding structures for H and CH_3 along side with these species on the icosahedral Ni_{13} cluster correspondingly. Numbers denote the bond lengths. For both H and CH_3 on

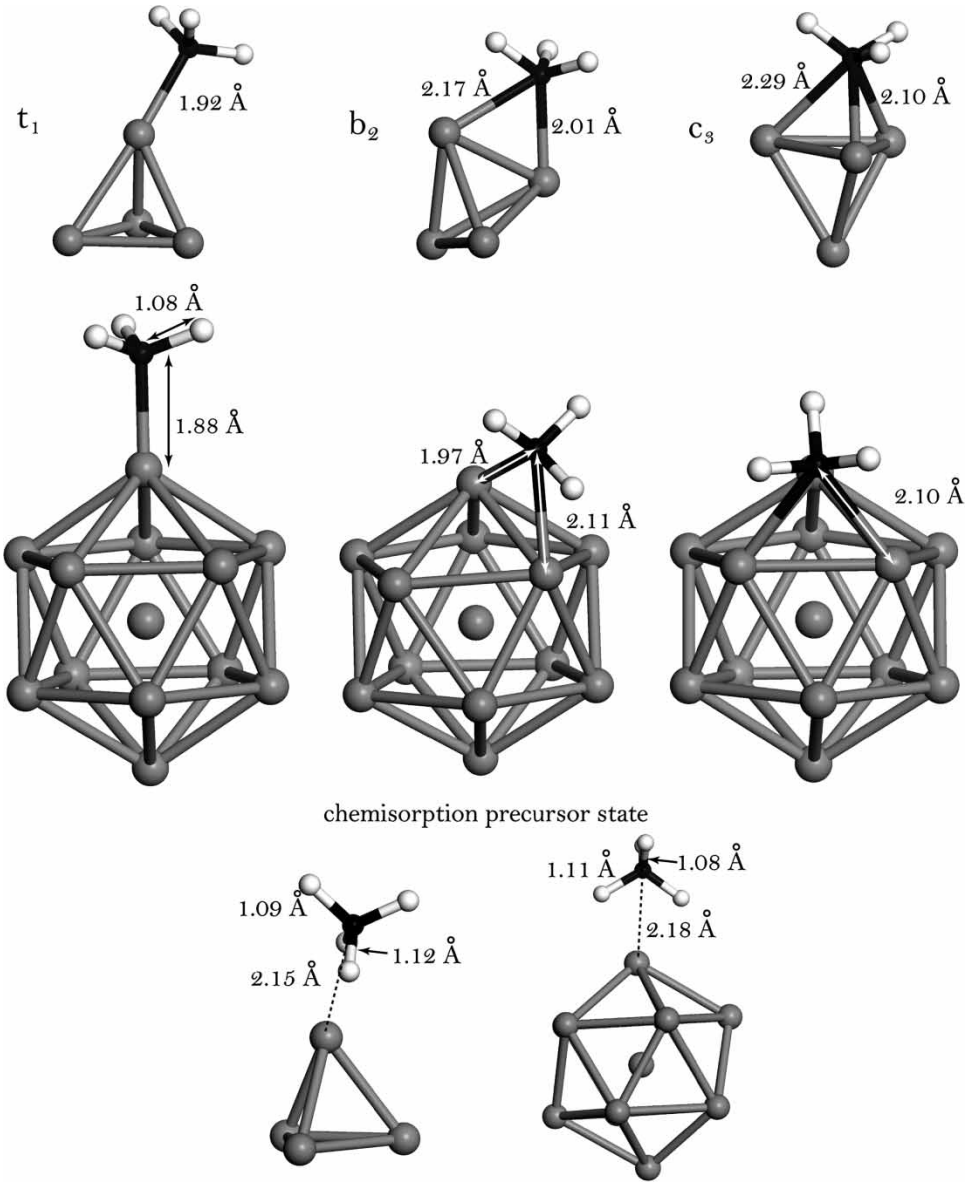

Figure 6. The adsorption of CH_3 on the t_1, b_2 and c_3 site of Ni_4 and the icosahedral Ni_{13} cluster. The chemisorption state of CH_4 on these two clusters are also shown.

Ni_4, t_1 and b_2 are the favoured binding sites, whereas c_3 site is not stable and adsorbates tend to migrate to the b_2 site eventually. However on Ni_{13}, the c_3 is the most favourable site for H binding, t_1 site for CH_3.

The dissociation behaviours of hydrogen and methane were also studied by letting these molecules approach the t_1 and b_3 sites of the Ni_{13} cluster [4]. The chemisorption precursor states were observed for both hydrogen and methane at the t_1 site, as illustrated by Figures 5 and 6. This bears a striking resemblance between two clusters.

When H_2 molecule was examined, it was found that H_2 can molecularly adsorb at the t_1 site of Ni_4 tetrahedral cluster. Unlike the case with isolated nickel atom, hydrogen molecule maintained its structure, where H—H bond length is 0.86 Å. The TS search calculation showed that the dissociation barrier to break H—H is 3.7 kcal/mol. Two dissociated H atoms ended up binding with at the same nickel atom. The dissociation of methane on Ni_4 cluster into H and CH_3 was studied using the same approach. The dissociation barrier was found to be 12.4 kcal/mol. The H atom ended up at the b_2 site, while CH_3 bound at the t_1 site on the side of the cluster.

The chemisorption state of methane reduces its dissociation barriers (from ~18 down to 9.9 kcal/mol [4]) on nickel cluster when compared to Ni(1 1 1) surface. Unlike crystalline surfaces, the s and d orbitals on surface nickel atoms in the clusters provide an adsorption anchor point which could serve as a precursor for further adsorptions. For hydrogen molecules, the reactant state of dissociation is stabilised. Nevertheless, the bond formed between methane and the cluster surface draws these adsorbates closer to surfaces as opposed to planar surfaces. In general, the significance is that the molecular adsorption state eliminates the repulsion between hydrocarbons and surface and substantially lowers the dissociation barrier.

4. Conclusions

In this short study, we examined the interactions between an isolated nickel atom with hydrogen and methane molecules. The stable geometry of H—Ni—H was found to be bent and in a singlet ground state. Similar results were found for hydrocarbons, such as, methane, ethane etc. This is consistent with other DFT studies and further demonstrates the shortcomings of results obtained with Hartree–Fock methods. The H—H and H—C bonds can be easily stretched and broken in the presence of nickel atoms. The s and d orbitals of un-bonded nickel atom allowed nickel to attach to these molecules and even changed structure hydrogen molecule.

More coordinated nickel atoms in a cluster environment were also studied. The Ni_4 tetrahedral cluster was used as one such model. Although cluster provides nickel with a more stable, less chemically active setting, there are still available s and d orbitals that give rise to a molecular adsorption of hydrogen and methane on the t_1 site of the clusters. However, nickel in this case is unable to break H—H and H—C bonds and activation barriers were observed.

Acknowledgements

This work was partially supported by the US Department of Energy, Office of Science, Grant DE-ER9542165. The calculations conducted in this work were also supported in part by the Golden Energy Computing Organization at the Colorado School of Mines using resources acquired with financial assistance from the National Science Foundation and the National Renewable Energy Laboratory.

References

[1] C. Burda, X.B. Chen, R. Narayanan, and M.A. El-Sayed, *Chemistry and properties of nanocrystals of different shapes*, Chem. Rev. 105 (2005), pp. 1025–1102.
[2] N. Tian, Z.Y. Zhou, S.G. Sun, Y. Ding, and Z.L. Wang, *Synthesis of tetrahexahedral platinum nanocrystals with high-index facets and high electro-oxidation activity*, Science 316 (2007), pp. 732–735.
[3] R. Narayanan and M.A. El-Sayed, *Shape-dependent catalytic activity of platinum nanoparticles in colloidal solution*, Nano Lett. 4 (2004), pp. 1343–1348.
[4] B. Liu, M.T. Lusk, and J.F. Ely, *The influence of nickel catalyst geometry on the dissociation barriers of H_2 and CH_4: Ni_{13} vs. Ni_{13} vs. Ni(111)*, J. Phys. Chem. C (in press).
[5] B. Delley, *An all-electron numerical method for solving the local density functional for polyatomic molecules*, J. Chem. Phys. 92 (1990), pp. 508–517.
[6] B. Delley, *From molecules to solids with the DMol^3 approach*, J. Chem. Phys. 113 (2000), pp. 7756–7764.
[7] J.P. Perdew, *Electronic Structure of Solids '91*, Akademie Verlag, Berlin, 1991.
[8] J.P. Perdew and Y. Wang, *Accurate and simple analytic representation of the electron-gas correlation energy*, Phys. Rev. B 45 (1992), pp. 13244–13249.
[9] S.W. Lin, S.C. Chang, R.S. Liu, S.F. Hu, and N.T. Jan, *Fabrication and magnetic properties of nickel nanowires*, J. Magn. Magn. Mater. 282 (2004), pp. 28–31.
[10] D.R. Hamann, M. Schluter, and C. Chiang, *Norm-conserving pseudopotentials*, Phys. Rev. Lett. 43 (1979), pp. 1494–1497.
[11] P. Pulay, *Convergence acceleration of iterative sequences – the case of SCF iteration*, Chem. Phys. Lett. 73 (1980), pp. 393–398.
[12] M.P. Guse, R.J. Blint, and A.B. Kunz, *Potential energy curves for NiH and NiH_2*, Int. J. Quantum Chem. XI (1977), pp. 725–732.
[13] M.R.A. Blomberg and P.E.M. Siegbahn, *An important bound singlet-state of NiH_2*, J. Chem. Phys. 78 (1983), pp. 986–987.
[14] Jaguar, version 6.0, Schrodinger, LLC (2005).
[15] M.R.A. Blomberg and P.E.M. Siegbahn, *Singlet and triplet energy surfaces of NiH_2*, J. Chem. Phys. 78 (1983), pp. 5682–5692.
[16] M. Blomberg, U. Brandemark, L. Pettersson, and P. Siegbahn, *Contracted CI calculations of models for catalytic reactions involving transition-metals*, Int. J. Quantum Chem. 23 (1983), pp. 855–863.
[17] F. Ruette, G. Blyholder, and J. Head, *Bonding and potential-energy curves for NiH and NiH_2*, J. Chem. Phys. 80 (1984), pp. 2042–2048.
[18] S. Li, J. VanZee, W. Weltner, M.G. Cory, and M.C. Zerner, *Magneto-infrared spectra of matrix-isolated NiH and NiH_2 molecules and theoretical calculations of the lowest electronic states of NiH_2*, J. Chem. Phys. 106 (1997), pp. 2055–2059.

[19] J.R. Barron, A.R. Kelley, and R.F. Liu, *NiH_2 has a singlet ground state*, J. Chem. Phys. 108 (1998), pp. 1–3.
[20] M. Barysz and M.G. Papadopoulos, *On the ground state of NiH_2*, J. Chem. Phys. 109 (1998), pp. 3699–3700.
[21] G.C. Bond, *Catalysis by Metals*, Academic Press, New York, 1962.
[22] D.H. Dowden, *Chemisorption and Valency*, *in Chemisorption*, Academic Press, New York, 1957.
[23] M.R.A. Blomberg, U. Brandemark, and P.E.M. Siegbahn, *Theoretical investigation of the elimination and addition reactions of methane and ethane with nickel*, J Am. Chem. Soc. 105 (1983), pp. 5557–5563.
[24] H. Burghgraef, A.P.J. Jansen, and R.A.v. Santen, *Theoretical investigation of the insertion of nickel in the CH bond of CH_4. Electronic structure calculations and dynamics*, J. Chem. Phys. 98 (1993), pp. 8810–8818.
[25] H.A. Jahn and E. Teller, *Stability of polyatomic molecules in degenerate electronic states I. Orbital degeneracy*, Proc. R. Soc. Lond. Ser. A Math. Phys. Sci. 161 (1937), pp. 220–235.
[26] K.P. Huber and G. Herzberg, *Molecular Spectra and Molecular Structure IV, Constants of Diatomic Molecules*, Van Nostrand, New York, 1979.